

VALIDATION OF MULTIAXIAL FATIGUE MODELS FOR STRUCTURAL STEELS

L. Reis¹, B. Li² and M. Freitas³

¹ Dept. Engenharia Mecânica, Instituto Superior Técnico,
Av. Rovisco Pais, 1049-001 Lisboa, Portugal
E-mail: lreis@ist.utl.pt
Tfno: 351 218417481 Fax: 351 218147915

² Dept. Engenharia Mecânica, Instituto Superior Técnico,
Av. Rovisco Pais, 1049-001 Lisboa, Portugal
E-mail: bli@ist.utl.pt
Tfno: 351 218419480 Fax: 351 218147915

³ Dept. Engenharia Mecânica, Instituto Superior Técnico,
Av. Rovisco Pais, 1049-001 Lisboa, Portugal
E-mail: mfreitas@dem.ist.utl.pt
Tfno: 351 218417459 Fax: 351 218147915

RESUMEN

Existem vários modelos sobre fadiga multiaxial propostos na literatura. Alguns deles foram desenvolvidos para determinar a amplitude da tensão de corte sob condições de carregamento em fadiga multiaxial. Uma eficiente análise em fadiga de componentes e estruturas submetidas a carregamento multiaxial requer a validação de modelos e abordagens apropriadas. Neste artigo são apresentados o trabalho experimental e teórico realizados sobre o comportamento mecânico do aço estrutural 42CrMo4, temperado e revenido, em fadiga multiaxial. Os ensaios foram realizados utilizando uma máquina servo-hidráulica biaxial (8800 Instron) no regime de fadiga a elevado número de ciclos, $10^5 - 10^6$ ciclos. Foram consideradas quatro trajetórias de carregamento, compostas por tracção/torção cíclicas com diferentes rácios entre a componente normal e de corte, mantendo a mesma tensão equivalente de von Mises. Posteriormente os resultados experimentais obtidos em fadiga são analisados e correlacionados por um parâmetro de fadiga, o qual avalia num novo espaço da tensão de corte. A abordagem da Menor Elipse Circunscritiva (MEC) é utilizada para determinar a amplitude da tensão de corte, obtendo-se uma correlação interessante.

ABSTRACT

There are many multiaxial fatigue models proposed in the literature, and many corresponding approaches have been developed for evaluating the shear stress amplitude under multiaxial fatigue loading conditions. For efficient computational fatigue analysis of components and structures, it is required to carry out further validations of multiaxial fatigue models and appropriate approaches for shear stress evaluation under service loading conditions. In this paper, systematic fatigue experiments are presented for a structural steel, 42CrMo4, under typical axial-torsional multiaxial loading paths. Tests were carried out in high cycle fatigue regime, $10^5 - 10^6$ cycles. The same von Mises equivalent stress was applied in different loading paths with several ratios of shear stress/normal stress. Then the experimental fatigue life results are analysed and correlated with the fatigue damage parameter which were evaluated in the new proposed shear stress space. The MCE approach is used for evaluating the shear stress amplitude and improved correlations are shown.

ÁREAS TEMÁTICAS PROPUESTAS: Técnicas Experimentales, Aplicaciones Prácticas en Ingeniería.

PALABRAS CLAVE: Fatigue strength, Life prediction, Multiaxial fatigue.

1. INTRODUCTION

Most components and structures in industry are generally subjected to multiaxial stress states, which can occur either due to multiaxial loading or to local induced multiaxial stress states (on notches, on contact points, etc.) or due to residual stress states due to machining, etc. There are many multiaxial fatigue models proposed in the literature, and many corresponding approaches have been developed for

evaluating the shear stress amplitude under multiaxial fatigue loading conditions [1]. For efficient computational fatigue analysis of components and structures, it is required to carry out further validations of multiaxial fatigue models and appropriate approaches for shear stress evaluation under service loading conditions. In this paper, systematic fatigue experiments are presented for a structural steel, 42CrMo4, quenched and tempered steel, under typical axial-torsional multiaxial loading paths. Tests were carried out in high

cycle fatigue regime, $10^5 - 10^6$ cycles. The same von Mises equivalent stress was applied in different loading paths. Within those, several ratios of shear stress/normal stress were considered.

For structural steels, the shear stress amplitude is one of the important parameters in the formulations of multiaxial fatigue damage models. Conventionally, the shear stress amplitude was usually evaluated in the shear stress space based on the von Mises equivalence ($\tau = \sigma / \sqrt{3}$) or the Tresca equivalence ($\tau = \sigma / 2$) for the multiaxial loading conditions. However, the relationship of the equivalent shear stress related to the axial stress component may vary significantly depending on the type of the material. For example, the ratio of the torsion fatigue limite over the bending fatigue limite τ_{-1} / σ_{-1} varies from 0.5 for mild metals to 1 for brittle metals [2].

In this paper it is proposed to evaluate the shear stress amplitude in the stress space appropriate to the material type. For the 42CrMo4 steel studied, the shear stress space with the equivalence ($\tau = 0.65 * \sigma$) is used for the shear stress amplitude evaluations under multiaxial loading conditions. The MCE (Minimum Circumscribed Ellipse) approach, developed by the authors previously [3], is used for evaluating the shear stress amplitude and experimental results are correlated. Better correlations are shown.

2. MATERIAL DATA, SPECIMEN FORM AND TEST PROCEDURE

The material studied in this paper is the high strength steel 42CrMo4. The chemical composition is shown in table 1. In order to characterize the cyclic stress-strain behavior of the materials studied, tension-compression low cycle fatigue tests were carried out. Monotonic and cyclic mechanical properties are shown in table 2 (cyclic properties obtained by fitting the test results). The geometry and dimensions of the specimen are shown in figure 1.

C	Si	Mn	P	Cr	Ni	Mo	Cu
0.39	0.17	0.77	0.025	1.10	0.30	0.16	0.21

Table 1. Chemical composition of the material studied 42CrMo4 (in wt%)

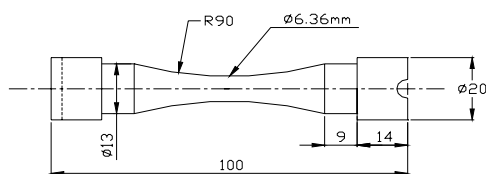


Figure 1. Specimen geometry for biaxial cyclic tension-compression with cyclic torsion tests

Tensile strength	σ (MPa)	1100
Yield strength	$\sigma_{0.2, \text{monotonic}}$ (MPa)	980
Elongation	A (%)	16
Young's modulus	E (GPa)	206
Yield strength	$\sigma_{0.2, \text{cyclic}}$ (MPa)	540
Strength coefficient	K' (MPa)	1420
Strain hardening exponent	n'	0.12
Fatigue strength coefficient	σ_f' (MPa)	1154
Fatigue strength exponent	b	-0.061
Fatigue ductility coefficient	ϵ_f'	0.18
Fatigue ductility exponent	c	-0.53

Table 2. Monotonic and cyclic mechanical properties of the material studied

To study the effects of the multiaxial loading paths and in particular both the axial component and the torsional component on the fatigue life, a series of loading paths were applied in the experiments as shown in table 3.

The tests of biaxial cyclic tension-compression with cyclic torsion were performed by a biaxial servo-hydraulic machine, shown in figure 2. Test conditions were as follows: frequency 4-6 Hz at room temperature and laboratory air. Tests ended up when the specimens were completely broken.

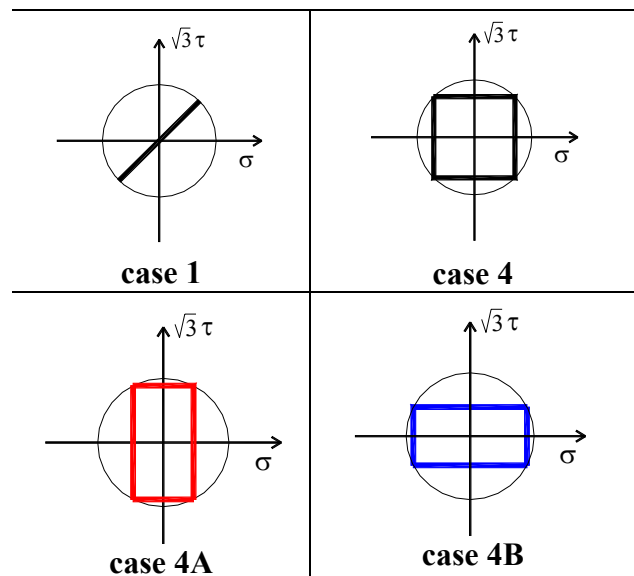


Table 3. Multiaxial fatigue loading paths

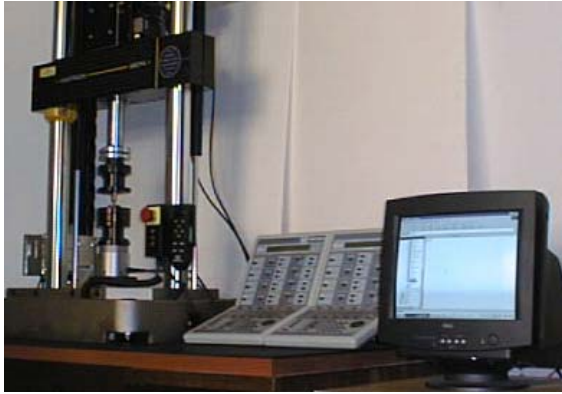


Figure 2. Biaxial test machine (Instron 8874)

3. THEORETICAL ANALYSIS OF THE FATIGUE LIFE

Many multiaxial fatigue models have been proposed in the last decades [1], the shear stress amplitude is one of the important parameters in the formulations of the multiaxial fatigue damage models.

3.1 Equivalent Strain Range of ASME Code

The ASME Boiler and Pressure Vessel code Procedure [4] is based on the von Mises hypothesis, but employs the strain difference $\Delta\epsilon_i$ between time t_1 and t_2 :

$$\Delta\epsilon_{eq} = \frac{1}{(1+\nu)\sqrt{2}} \left\{ (\Delta\epsilon_x - \Delta\epsilon_y)^2 + (\Delta\epsilon_y - \Delta\epsilon_z)^2 + (\Delta\epsilon_z - \Delta\epsilon_x)^2 + \frac{3}{2} (\Delta\epsilon_{xy}^2 + \Delta\epsilon_{yz}^2 + \Delta\epsilon_{xz}^2) \right\}^{1/2} \quad (1)$$

where the equivalent strain range $\Delta\epsilon_{eq}$ is maximized with respect to time.

Eq. (1) produces a lower equivalent strain range for out-of-phase than the in-phase loading, predicting an increase of the fatigue life, which is in contradiction with experimental results.

3.2. An Improved Model Based on the ASME Code

The ASME Code approach expressed in Eq. (1), defines a parameter which has a drawback that is, it produces a lower equivalent strain range for non-proportional than the proportional loading, which underestimates the fatigue damage of non-proportional loading, since many recent experiments have shown that the non-proportional loading reduce the fatigue life significantly than the proportional loading with the same loading amplitude.

An improved model based on the ASME code approach is proposed by considering the additional hardening and correcting the strain range parameter for non-proportional loading path:

$$\Delta\epsilon_{NP} = (1 + \alpha F_{NP}) \Delta\epsilon_{eq} \quad (2)$$

where F_{NP} is the non-proportionality factor of the loading path, α is a material constant of additional hardening, $\Delta\epsilon_{eq}$ is the strain range parameter calculated by Eq.(1), and $\Delta\epsilon_{NP}$ is the corrected strain range parameter.

Eq. (2) is similar with the approach proposed by Itoh et al. [5], but here the MCE (minimum circumscribed Ellipse) approach developed by M. de Freitas et al [3] previously is applied for evaluating the non-proportionality factor of the loading path.

Then the Manson-Coffin formulation can be used for life predictions:

$$\frac{\Delta\epsilon_{NP}}{2} = \frac{\sigma'_f - \sigma_m}{E} (2N_f)^b + \epsilon'_f (2N_f)^c \quad (3)$$

where σ_m is the mean stress, E is the young's modulus, σ'_f is the fatigue strength coefficient, ϵ'_f is the fatigue ductility coefficient, and b and c are fatigue strength and fatigue ductility exponents, respectively.

3.3. MCE Approach for evaluating shear stress amplitude

Among many multiaxial models, the Sines [6] and the Crossland [7] are two important criteria, which are formulated by the amplitude of the second deviatoric stress invariant and the hydrostatic stress P_H :

$$\sqrt{J_{2,a}} + k(N)P_H = \lambda(N) \quad (4)$$

Crossland suggested using the maximum value of the hydrostatic stress $P_{H,max}$ instead of the mean value of hydrostatic stress $P_{H,m}$ used by Sines in the Eq.(4). A physical interpretation of the criterion expressed as Eq.(4) is that for a given cyclic life N, the permissible amplitude of the root-mean-square of the shear stress over all planes is a linear function of the normal stress averaged over all planes. Besides, from the viewpoint of computational efficiency, the stress-invariant based approach such as Eq. (4) is easy to use and computationally efficient.

In practical engineering design, the Sines and Crossland criteria have found successful applications for proportional multiaxial loading. For non-proportional multiaxial loading, it has been shown that the Sines and Crossland criteria can also yield better prediction results by using improved method MCE for evaluating the effective shear stress amplitude of the non-proportional loading path.

The evaluation of shear stress amplitude is a key issue for fatigue estimations using Eq. (4). The definition of the square root of the second invariant of the stress deviator is:

$$\sqrt{J_2} \equiv \sqrt{\frac{1}{6}\{(\sigma_{xx} - \sigma_{yy})^2 + (\sigma_{yy} - \sigma_{zz})^2 + (\sigma_{zz} - \sigma_{xx})^2\}} + \sqrt{\{(\sigma_{xy})^2 + (\sigma_{yz})^2 + (\sigma_{zx})^2\}} \quad (5)$$

One direct way to calculate the amplitude of $\sqrt{J_2}$ is:

$$\sqrt{J_{2,a}} \equiv \sqrt{\frac{1}{6}\{(\sigma_{xx,a} - \sigma_{yy,a})^2 + (\sigma_{yy,a} - \sigma_{zz,a})^2 + (\sigma_{zz,a} - \sigma_{xx,a})^2\}} + \sqrt{\{(\sigma_{xy,a})^2 + (\sigma_{yz,a})^2 + (\sigma_{zx,a})^2\}} \quad (6)$$

Eq.(6) is applicable for proportional loading, where all the stress components vary proportionally. However, when the stress components vary non-proportionally (for example, with phase shift between the stress components), Eq.(6) gives the same result with that of proportional loading condition. In fact, the non-proportionality has influence on the shear stress amplitude generated by multiaxial loading. Therefore, a new methodology is needed.

The longest chord (LC) approach is one of the well-known approaches as summarized by Papadopoulos [2], which defines the shear stress amplitude as half of the longest chord of the loading path, denoted as D/2.

The MCC approach [2] defines the shear stress amplitude as the radius of the minimum circle circumscribing to the loading path. On the basis of MCC approach, a new approach, called the minimum circumscribed ellipse (MCE) approach [3], was proposed to compute the effective shear stress amplitude taking into account the non-proportional loading effect. The load traces are represented and analyzed in the transformed deviatoric stress space, where each point represents a value of $\sqrt{J_2}$ and the variations of $\sqrt{J_2}$ are shown during a loading cycle. The schematic representation of the MCE approach and the relation with the minimum circumscribed circle (MCC) approach are illustrated in figure 3:

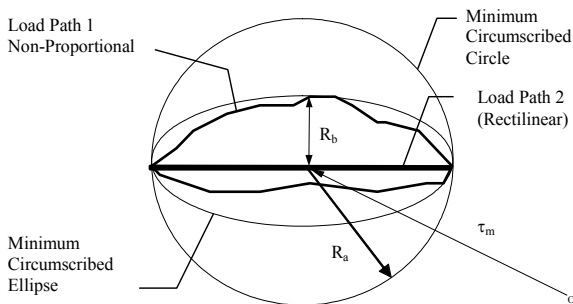


Figure 3. The MCC and MCE circumscribing to shear stress traces, R_a and R_b are the major and minor radius of MCE, respectively.

The idea of the MCE approach is to construct a minimum circumscribed ellipse that can enclose the whole loading path throughout a loading block in the transformed deviatoric stress space. Rather than defining $\sqrt{J_{2,a}} = R_a$ by the minimum circumscribed circle (MCC) approach, a new definition of was proposed [3], where R_a and R_b are the lengths of the major semi-axis and the minor semi-axis of the minimum circumscribed ellipse respectively.

The ratio of R_b/R_a represents the non-proportionality of the shear stress path. The important advantage of this new MCE approach is that it can take into account the non-proportional loading effects in an easy way.

As shown in figure 3, for the non-proportional loading path 1, the shear stress amplitude is defined as:

$$\sqrt{J_{2,a}} = \sqrt{R_a^2 + R_b^2} \quad (7)$$

For the proportional loading path 2, it is defined as $\sqrt{J_{2,a}} = R_a$ since R_b is equal to zero (rectilinear loading trace).

4. NUMERICAL ANALYSES

4.1 Finite Element Meshing

The ABAQUS element type isoparametric solid element C3D20R with 20 nodes and reduced integration points was used. Full model was meshed in this study due to two reasons: a) under combined axial/torsion loadings, no symmetry condition can be used, b) to study the interactions among the material elements in plastic deformations and stress redistributions. Figure 4 shows the FE model. The mesh contains 1944 elements and 8809 nodes.

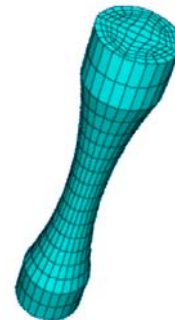


Figure 4. FE mesh for specimen

4.2 Incremental Plasticity Procedure

The cyclic loading sequences shown in table 3 were divided as 32 discrete time steps for one loading cycle. The simulations were based on the incremental plasticity procedure. Since the full model is meshed with a large amount of elements, the computation is very time consuming. Since the plasticity and fatigue

damage process are path dependent, the simulations based on the incremental procedures should be used. A recent multiaxial fatigue prediction method EVICD (EVENt INdependent Cumulative Damage) [8] works also incrementally, the damage evaluation is based on the plastic work and the normal stress on the instantaneous maximum shear stress plane or on octahedral planes.

4.3 Additional hardening coefficient α

For non-proportional straining, a rotation of the principal strain axes leads to an additional cyclic strain hardening and higher than that obtained under stable conditions for proportional stressing. In the latter case, dislocations glide on a fixed set of slip planes, whereas for continuously rotating principal axes, many slip systems are activated. Therefore an additional factor must be introduced to represent this extra hardening. This parameter is described in detail in reference [9].

5. RESULTS AND DISCUSSIONS

5.1 FEM - cyclic stress-strain behavior under proportional and non-proportional loading

The simulations by FEM based incremental plasticity analyses for multiaxial cyclic loading are computationally very time consuming and also the problem with iteration convergence may occur in the computation process. The preliminary results showed that the stress-strain responses reach a stabilized cyclic state after 2~3 loading cycles, by using the kinematic hardening rule in the present study. The influences of the loading paths on the cyclic stress-strain responses were shown. The cutting-view images of stress/strain distributions inside the component at different time step of the loading cycle are helpful to study the evolutions and redistributions of the cyclic stress/strain fields. The stress-strain ranges of the stabilized cycle can be used for life predictions. Figures 5, 6 and 7 show stress (S22) - strain (E22) evolutions history of square, rectangle down and rectangle up loading paths.

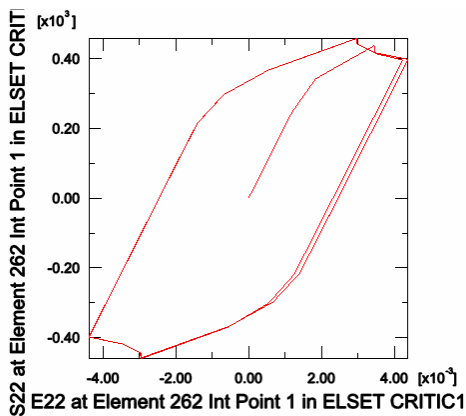


Figure 5. Square loading path - case 4.

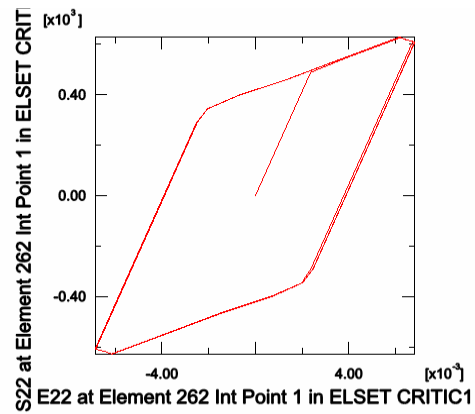


Figure 6. Rectangle down loading path - case 4B.

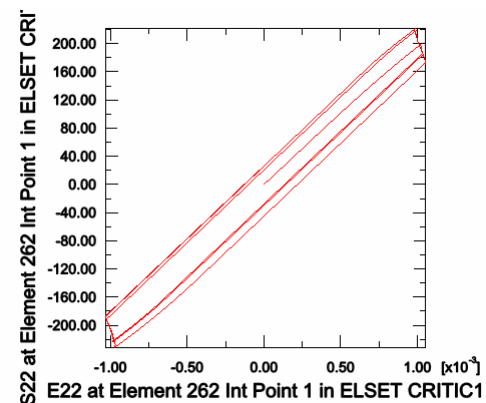


Figure 7. Rectangle up loading path - case 4A.

The influence of the loading path on mechanical behavior (response) and the correspondent stress-strain evolution are demonstrated. To the same equivalent von Mises stress the dissipated energy for each case is different. As can be observed from figure 7, case 4A - rectangle up, the internal area of the hysteresis loop is smaller than the other two cases, which means that in this case less energy is dissipated and a bigger number of cycles is expected. Concerning this parameter (dissipated energy) the rectangle down, figure 6, is the case where more energy is dissipated. These results demonstrate the big influence of each component, axial and torsional, in the definition of the loading path.

Other results, in terms of different components as shear stress, shear strain, equivalent plastic strains were obtained from the FE program. It was shown that the most stressed material element has strong interactions with its neighboring elements by plastic deformation and stress redistribution.

5.2 Experimental cyclic stress-strain behavior under proportional and non-proportional loading

Proportional cyclic tests were conducted in the plane $(\sigma, \sqrt{3}\tau)$. Non-proportional cyclic tests were conducted with the square, rectangle up and rectangle down loading paths, respectively (see table3). Figure 8 shows the evolution of experimental life with equivalent v. Mises stress.

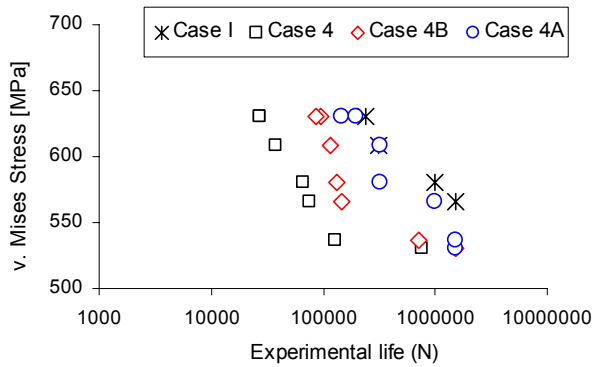


Figure 8. Evolution of experimental life with equivalent von Mises stress.

From figure 8 it is possible to conclude that the square loading path is the most severe in terms of fatigue life and the proportional case (case I) the least one. Can also be observed that the case 4A (rectangle up) is quite close to the case I. This means that a bigger torsional component, compared with axial one, has not strong influence in the fatigue life. In the middle of the results mentioned before appears the case 4B, which show that the axial component has a big influence in the fatigue life. Besides, figure 8 shows bigger scatter in the correlations of the von Mises stress with the experimental life.

In order to get better correlations, the new shear stress space parameter with the equivalence ($\tau=0.65*\sigma$) is used for the shear stress amplitude evaluations under multiaxial loading conditions. The parameter ($Ta+Sig_h$) is obtained from Eq. (4) with the shear stress amplitude calculated from Eq. (7). Figure 9 shows the evolution of the fatigue parameter with experimental life. The analysis allow to conclude that there are two tendencies, i.e. the proposed parameter correlates the 4 cases in two separate ways, one for cases 4 and 4A and another one for cases I and 4B.

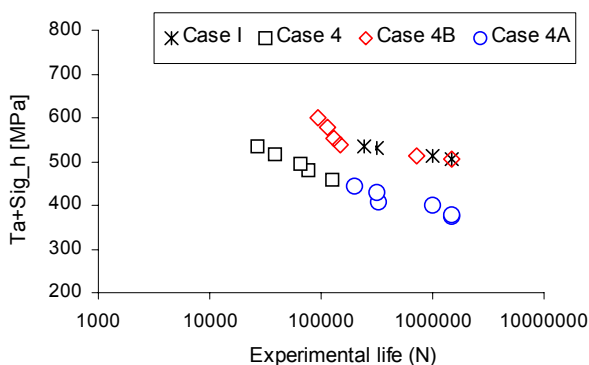


Figure 9. Evolution of the fatigue parameter with experimental life.

6. CONCLUSIONS

The simulations by the incremental plasticity procedures give very helpful insights to understand the

evolutions and redistributions of the cyclic stress/strain field under multiaxial loading conditions.

Experimental results show that the ratio between normal stress component and shear stress component has a strong influence to fatigue damage and consequently in fatigue life.

The shear stress space used for the evaluation of the shear stress amplitude of multiaxial loading conditions should be appropriate for the material type.

ACKNOWLEDGEMENTS

Financial support from the Fundação para Ciência e Tecnologia (FCT) is acknowledged.

REFERENCES

- [1] Socie D. F. and Marquis G. B. *Multiaxial Fatigue*, SAE, Warrendale, PA 15096-0001, 2000.
- [2] Papadopoulos, I.V., Davoli, P., Gorla, C., Fillipini, M. and Bernasconi, A. A comparative study of multiaxial high-cycle fatigue criteria for metals. *IJF*, Vol. 19, N°3, pp. 219-235.
- [3] M. de Freitas, B. Li and J.L.T. Santos, *Multiaxial Fatigue and Deformation: Testing and Prediction*, ASTM STP 1387, S. Kaluri and P.J. Bonacuse, Eds., ASTM, West Consh, 2000, PA, pp.139-156.
- [4] ASME Code Case N-47-23 (1988) Case of ASME Boiler and Pressure Vessel Code, ASME.
- [5] Itoh, T. and Miyazaki, T., A damage model for estimating low cycle fatigue lives under non-proportional multiaxial loading, *Proc. of the 6th Int. Conf. on Biaxial/Multiaxial Fat. & Fract*, Ed. by M. de Freitas, Lisbon, June 25-28, 2001, pp. 503-510.
- [6] Sines, G., (1959) *Metal Fatigue*, (edited by G. Sines and J.L.Waisman), McGraw Hill, N.Y, pp.145-169.
- [7] Crossland, B., (1956) *Proc. Int. Conf. on Fatigue of Metals*, Inst. of Mech. Eng, London, pp.138-149.
- [8] Nowack H, Baum C, Ott W, Buczynski A, Glinka G. Achievements of the incremental multiaxial fatigue prediction method EVICD, *Proc. of the fifth Int. Conf. on LCF*, ed. by Portella, Sehitoglu and Hatanaka, Berlin, Germany, Sep. 9-11, 2003:277-282.
- [9] L. Reis, B. Li and M. de Freitas. *Biaxial Low-Cycle Fatigue for Proportional and Non-Proportional Loading Paths.*, *Proc. of the fifth Int. Conf. on LCF*, ed. by Portella, Sehitoglu and Hatanaka, Berlin, Germany, Sep. 9-11, 2003:265-270.